Paper 285

Proceedings of the Eleventh International Conference
on Computational Structures Technology,
B.H.V. Topping, (Editor),
Civil-Comp Press, Stirlingshire, Scotland

Spectrum-Compliant Accelerograms through Harmonic Wavelet Transform

D. Cecini and A. Palmeri
School of Civil and Building Engineering
Loughborough University, England

Abstract

Code-compliant accelerograms adopted for time-history dynamic analyses are required to be compatible with the elastic design spectrum defining the seismic action. The problem then arises to generate spectrum-compatible accelerograms while maintaining realistic non-stationary characteristics, which in turn may play an important role in the non-linear seismic response. In this paper, the harmonic wavelet analysis is resorted to as a potent tool to: first, deterministically modify an accelerogram to match the target spectrum; second, to randomly generate an arbitrary number of signals with the same non-stationary characteristics of the parent accelerogram.

Keywords: artificial accelerograms, earthquake engineering, harmonic wavelet transform, signal processing, spectrum-compatible accelerograms.

1 Introduction

Building codes define the seismic action through the elastic design spectrum (EDS), which is a way to represent synthetically the seismic hazard at a given site. Furthermore, the response spectrum analysis is widely recognised as the reference method of analysis and design for conventional earthquake-resistant structures. In order to achieve a superior level of understanding of the structural and non-structural response, however, non-linear time-history analysis has to be preferred. Such analysis is particularly useful for non-conventional buildings, when the inelastic behaviour of the structural components must be accurately modeled and cannot be simply accounted for with the behaviour factor q. One of the key issues with the non-linear time-history analysis is the selection of an appropriate set of seismic inputs [1]. International codes allow using both natural and artificial time-histories of ground accelerations but, besides generic prescriptions of being representative of the site hazard from a seismo-

logical standpoint, their on-average spectrum-compatibility is required: that is, if the elastic response spectrum (ERS) is computed for each accelerogram of the suite, the mean value of the spectral ordinates for each period of interest satisfies the compatibility conditions with the corresponding ordinate of the EDS, and therefore using this suite to run a linear-elastic time-history analysis will lead to the seismic response as the EDS prescribed by the code.

In this context, the direct use of natural accelerograms is an attractive option, but unfortunately they are often not available in a sufficient number at a given site to produce an acceptable structural assessment, therefore rising the need for artificial accelerograms. The latter can be either simulated signals or recorded accelerograms modified to cope with the required prescriptions. The EDS matching is not, however, a trivial prescription, mainly because the EDS given by seismic codes is a synthetic and indirect representation of the expected ground shaking at a given site under the design scenario (i.e. for given return period and soil conditions), while an accelerogram gives a direct representation of the seismic action. Importantly, the mapping between ERS and accelerograms is not bijective, since accelerograms provide richer information. Indeed, intensity, frequency content and duration of the ground shaking contribute altogether to build the ERS, but it is not possible to find them back: while a unique ERS can be computed from an accelerogram, an infinite number of accelerograms can be associated to a target EDS. It follows that some of these quantities must be specified to find the spectrum-compatible accelerograms (e.g. overall duration and energy content). In other words, the richer information allowed by the direct use of accelerograms, which is what makes worthwhile a non-linear time-history analysis even if computationally more demanding, must be provided apart from the EDS offered by the seismic code.

A number of different methods are available in the literature to simulate accelerograms (for a review see [2, 3]), the vast majority of them being stochastic, i.e. they deal with ground motion signals as samples of a non-stationary random process [4–9]. Nonetheless, accelerograms generated in this way are not always fully satisfactory, especially for geotechnical systems (e.g. Italian code NTC2008 bans their use) and for analyses where the energy content plays a crucial role ([10, 11]). Signal processing comes helpful then to analyses, generate and manipulate the accelerograms. A common practice is to use the Fourier Transform (FT) to look at the signals in the frequency domain, where the distribution of the seismic energy at different frequencies becomes apparent. On the other hand, the non-stationary characteristics of the accelerogram can be properly analysed in the time domain. As a matter of fact, time and frequency domains are in a kind of dualism because they are capable of highlighting some of the signal features while hiding some others. Joint time-frequency signal representations can be therefore deemed as a powerful strategy to analyse the evolutionary frequency content of accelerograms, and therefore getting the best from the two domains. Among them, the wavelet analysis [12] is a very promising tool, as it exploits localised functions (wavelets) instead of ever-lasting harmonics as a base to decompose a signal. The Harmonic Wavelet Transform (HWT) enjoys the additional advantage of overcoming the limitations of the classical FT without losing a meaning-

ful engineering interpretation in terms frequency content.

In this paper, a novel method based on the HWT is proposed to generate a set of spectrum-compatible accelerograms, which allow satisfying the compatibility conditions with a target EDS starting from a parent accelerogram while retaining the bulk of its non-stationary features in terms of amplitude and frequency. In a first stage, the parent accelerogram is deterministically modified in order to be spectrum-compatible. In a second stage, an arbitrary number of accelerograms is randomly generated, reproducing the joint time-frequency properties of the spectrum-compatibilised accelerogram. The numerical results demonstrate that the HWT can be successfully resorted to for solving the EDS generation problem while preserving the non-stationary characteristics of a given accelerogram.

2 Harmonic wavelet analysis

Wavelet analysis is a potent tool allowing a joint time-frequency representation of signals, therefore overcoming the main limitation of the classical Fourier analysis which does not possess time domain localisation capability. However, it must be stressed that the Heisenberg's uncertainty principle [12] defines a limit on the precision with which a signal can be simultaneously represented in time and frequency domain. The more the time domain detail is enhanced, the more the frequency one becomes poor, rising the need to find a compromise. The wavelet analysis consists of projecting the signal on a convenient basis of orthogonal functions, called wavelets, which can be generated by scaling and shifting a mother function (mother wavelet) [12]. In the continuous wavelet transform, the coefficient $a_{u,s}$ at scale s and position u of the signal $f(t)$ is given by:

$$a_{u,s} = \int_{-\infty}^{\infty} f(t)\, \overline{\psi_{u,s}}(t) \mathrm{d}t, \tag{1}$$

where the over-bar denotes the complex conjugate, while:

$$\psi_{u,s}(t) = \frac{1}{\sqrt{s}}\, \psi\left(\frac{t-u}{s}\right) \tag{2}$$

is the mother wavelet $\psi(t)$ scaled by the parameter $s \in \mathbb{R}^+$ (controlling the frequency distribution) and shifted by the parameter $u \in \mathbb{R}$ (localising the function at around $t = u$). The inverse continuous wavelet transform is given by:

$$f(t) = \frac{1}{C} \int_{-\infty}^{+\infty} \int_{0}^{+\infty} \frac{1}{s^2} a_{u,s}\, \psi_{u,s}(t)\, \mathrm{d}s\, \mathrm{d}u, \tag{3}$$

in which C is a normalisation constant.

Unlike a harmonic wave, which is an ever-lasting periodic function, a wavelet is a decaying function, and this feature gives to the wavelet analysis a time localisation capability. Interestingly, families of wavelets can be generated in a way to form

orthogonal bases, so that the wavelet transform is bijective, giving a unique representation for any signal. This is the case, for instance, of the harmonic wavelets proposed by Newland [13, 14], which are complex-valued functions with a box-shaped FT:

$$\Psi(\omega) = \mathrm{FT}\langle\psi(t)\rangle = \begin{cases} 1/2\pi & \text{for} \quad 2\pi \leq |\omega| < 4\pi; \\ 0 & \text{elsewhere.} \end{cases} \tag{4}$$

The corresponding complex valued harmonic mother wavelet in time domain is:

$$\psi(t) = \frac{\mathrm{e}^{i4\pi t} - \mathrm{e}^{i2\pi t}}{i\,2\pi\,t}. \tag{5}$$

It should be noted here that Eqs. (4) and (5) refer, without loss of generality, to the case of a signal of unitary time length, i.e. $0 \leq t \leq 1$, and therefore meaningful energy content for $\omega > 2\pi$.

The first discrete scheme proposed by Newland [13] to generate the whole family of orthogonal wavelets from the mother one is called dyadic, and comes from letting $s = 2^{-j}$, $u = 2^{-j}\,k$, namely changing the argument in Eq. (5) from t to $(2^j t - k)$:

$$\hat{\psi}_{j,k}(t) = \psi_{2^{-j}k,2^{-j}}(t) = \psi(2^j\,t - k), \tag{6}$$

where $j > 0$ and $k \in [0, 2^j]$ are integers, and the hat denotes the use of a discrete wavelet transform. By doing this, the shape of the wavelet is not changed but its horizontal scale is compressed by the factor 2^j, being j the level of the wavelet, while its position is translated by k units at the new scale. As we can see in Figure 1(a), at the generic level j, the wavelet's Fourier transform occupies the band from $2\pi\,2^j$ to $4\pi\,2^j$, which is j octaves higher up the frequency scale. The HWT coefficients are given by:

$$\hat{a}_{j,k} = 2^j \int_{-\infty}^{+\infty} f(t)\,\overline{\hat{\psi}_{j,k}(t)}\,\mathrm{d}t \tag{7}$$

and, since seismic signals are always real, the expansion (reconstruction) formula can be expressed as:

$$f(t) = 2\,\mathrm{Re}\left\{\sum_j \sum_{k=0}^{2^j} \hat{a}_{j,k}\,\hat{\psi}_{j,k}(t)\right\}, \tag{8}$$

where the first summation is intended over all j indexes. The second scheme proposed by Newland [14] leads to the generalised HWT. Instead of splitting the frequency axis into octave bands of increasing width, the whole set of band wavelets is generated by:

$$\hat{\psi}_{\{m,n\}}(t) = \frac{\mathrm{e}^{i\,n\,2\pi t} - \mathrm{e}^{i\,m\,2\pi t}}{i2\pi\,(n-m)\,t}, \tag{9}$$

which in the frequency domain corresponds to:

$$\hat{\Psi}_{\{m,n\}}(\omega) = \mathrm{FT}\langle\hat{\psi}_{\{m,n\}}(t)\rangle = \begin{cases} \frac{2\pi}{n-m} & \text{for } 2\pi\,m \leq \omega < \ 2\pi\,n; \\ 0 & \text{elsewhere.} \end{cases} \tag{10}$$

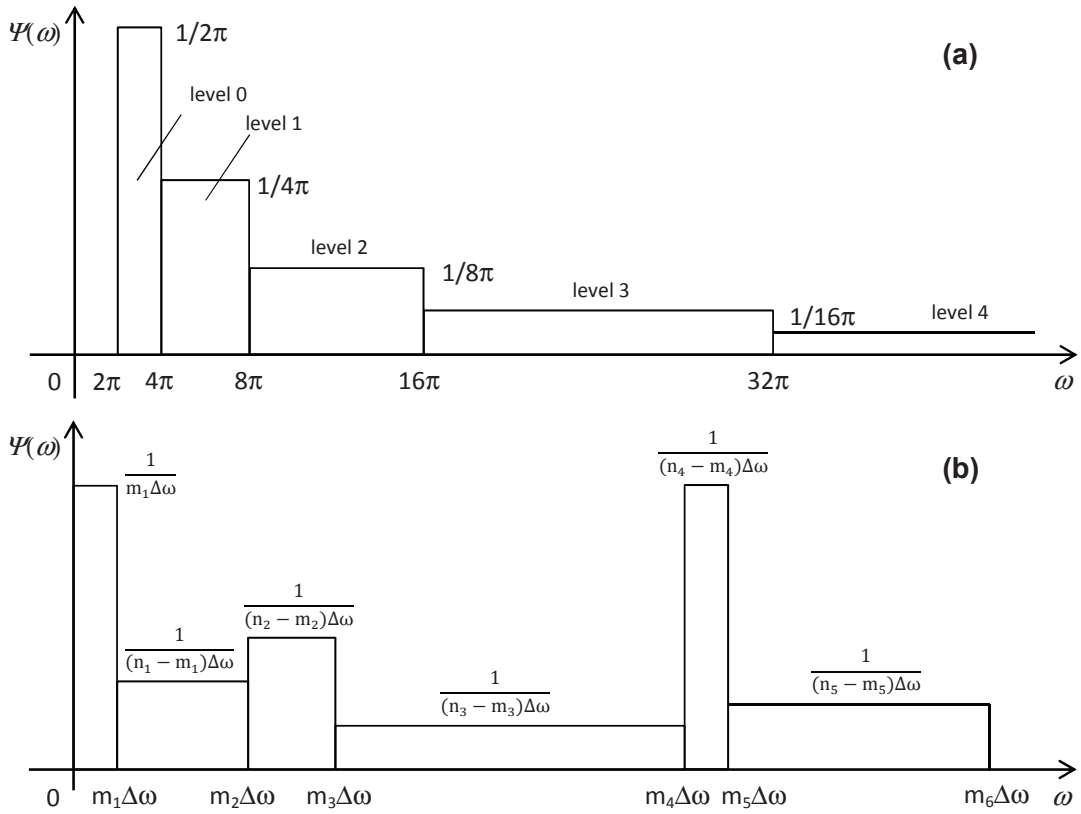

Figure 1: Representation in the frequency domain: (a) dyadic scheme; (b) an example of generalised scheme for harmonic wavelet base with non-overlapping intervals ($n_i = m_{i-1}$) of arbitrary bandwidth (adapted from Newland [14]).

Interestingly, if we put $m = 2^j$ and $n = 2^{j+1}$, we obtain again the dyadic scheme. Wavelet translation by a time step $k/(n-m)$ is achieved by:

$$\hat{\psi}_{\{m,n\},k}(t) = \frac{\mathrm{e}^{i\,n\,2\pi\left(t-\frac{k}{n-m}\right)} - \mathrm{e}^{i\,m\,2\pi\left(t-\frac{k}{n-m}\right)}}{i2\pi\,(n-m)\left(t-\frac{k}{n-m}\right)} = \hat{\psi}_{\{m,n\}}\left(t - \frac{k}{n-m}\right), \tag{11}$$

and in the frequency domain corresponds to a complex phase rotation:

$$\hat{\Psi}_{\{m,n\},k}(\omega) = \mathrm{FT}\langle\hat{\psi}_{\{m,n\},k}(t)\rangle = \begin{cases} \frac{2\pi}{n-m}\exp\left(\frac{-i\omega}{n-m}\,k\right) & \text{for } 2\pi\,m \le \omega < \ 2\pi\,n; \\ 0 & \text{elsewhere.} \end{cases} \tag{12}$$

Reconstruction formula is readily written (like Eq. (8)) as:

$$f(t) = 2\,\mathrm{Re}\left\{\sum_{\{m,n\}}\sum_{k=0}^{n-m} a_{\{m,n\},k}\;\hat{\psi}_{\{m,n\},k}(t)\right\}, \tag{13}$$

where the first summation is intended over all the $\{m, n\}$ pair. According to Newland [14], with this generalised scheme we can no longer talk about wavelet level j, while

we shall use the terminology level $\{m, n\}$ to denote a wavelet in the frequency band $2\pi\, m$ to $2\pi\, n$, where $n > m$, as it is apparent in Figure 1(b). To form a complete set of wavelets, adjacent levels must have box-shaped FTs touching each other but do not overlapping, so that all values of ω are included and no one is taken twice. Apart from this, there are no further rules about how to choose the $\{m, n\}$ pairs and hence divide the frequency axis. Importantly, while the unique scaling factor of the dyadic scheme relate the bandwidth and the central frequency of each level, the incorporation of an additional parameter in the generalised scheme provides more flexibility in the treatment of the signal.

Aimed at highlighting the key advantage of the HWT in comparison with the traditional FT, and therefore the reason for exploiting the HWT in this study, Fig. 2 offers the representation in both a joint time-frequency domain (top-row) and in the time domain only (second row) of a complex-valued harmonic wave (left column) and of a harmonic wavelet (right column). It can be seen that the harmonic wave is perfectly localised in the frequency domain (Fig. 2(a)), while being a periodic function no localisation is achieved in the time domain (Fig. 2(c)). The harmonic wavelet is still an unbounded function, as it decades with t^{-1}, but is well localised around $t = t_k$ (Fig. 2(d)), and in frequency domain does not occupy a single frequency, but a band spanning from ω_m to ω_n (Fig. 2(b)). When it comes to extract a component from a signal, the advantage of the HWT becomes apparent by comparing Figs. 2(g) and 2(h). In the first case, more harmonic waves are taken within the frequency band $[\omega_m, \omega_n]$ and it is not possible to localise their contribution in the time axis; in the second case, on the contrary, considering wavelets at the same level $\{m, n\}$ and centred in a given time interval allows a joint localisation in both time and frequency domain.

3 Spectral matching method

3.1 Position of the problem

The main goal in modifying a natural record to match a target EDS should be preserving as much as possible its features affecting the structural response. Unfortunately, depending on the type of analysis, there are many characteristics which could be considered, and the choice on which to focus is not unique. The proposed method aims to bring little modification, in terms of overall energy content, to fit the response spectrum into the zone bounded by the $90\% - 130\%$ of the target EDS. The lower bound is given by the code, prescribing spectral values to be at least 90% of the reference EDS, while the upper bound has been assumed as 130% of the target EDS, even if no specific provisions are given.

In order to minimise the modifications on the natural record of ground acceleration, the proposed method exploits the idea that, once the maximum response value has been reached by a single-degree-of-freedom (SDoF) oscillator of a given natural period T_j, what happens thereafter does not affect the response spectrum ordinate, and hence there is no reason to modify that part of the record. It follows that, to reach this

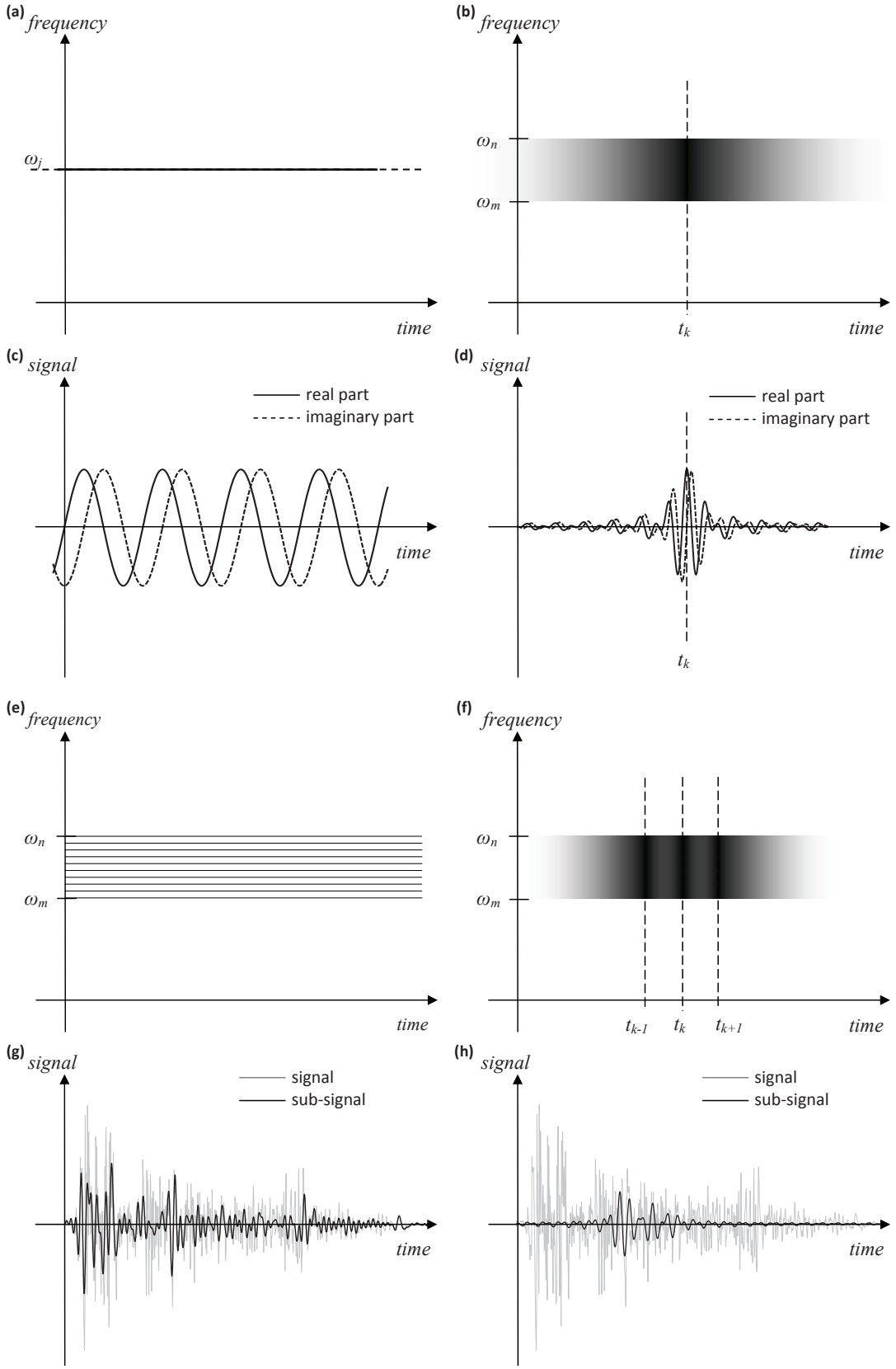

Figure 2: Single harmonic wave (a,c) versus single wavelet (b,d); sub-signal extraction by FT (e,g) versus HWT (f,h).

goal, we need to localise the instant τ_j at which the maximum response is achieved and then adjust the record surgically in the neighborhood of this time instant. Where the FT-based methods may bring adjustments localised in frequency domain only, the proposed method applies joint time-frequency localised modifications using the generalised HWT. According to Eq. (13), when the generic $\{m, n\}$ band in the frequency domain has to be modified, a set of $n - m$ k-indexed wavelets $\hat{\psi}_{\{m,n\},k}(t)$ are needed to fully re-construct this frequency sub-component of the signal $f(t)$. Letting t_f be the overall signal duration, the kth of these wavelets is centred at time $k/(n-m)\, t_f$. Since k goes from 0 to $n - m$, the first wavelet is centred at $t = 0$, while last one at $t = t_f$. It must be noticed that uncertainty principle holds, and thus the more precise localisation we have in the frequency domain by means of a narrow band, the less resolution we have in the time domain, with a longer time distance between the centres of two consecutive wavelets. Knowing when the maximum response is achieved by a SDoF system with a certain natural circular frequency $\omega_j = 2\pi/T_j$, the proposed procedure consists in modifying the coefficients of the two wavelets centred after and before that instant, along with the preceding coefficients covering the assumed time for the oscillator to reach its steady state response (or, if the maximum instant comes too close to the beginning of the record, all the coefficients coming before the maximum instant). For this purpose we will refer in the following to a time-of-(response)maximum (ToM) spectrum $S_{\text{ToM}}(T_j)$, defined as the time instant at which the generic SDoF oscillator of natural period T and a reference value of the viscous damping ratio ζ_0 takes the absolute maximum value.

Considering a SDoF with natural frequency ω_j and displacement $u_j(t)$, the equation of motion reads:

$$\ddot{u}_j(t) + 2\zeta_0\, \omega_j\, \dot{u}_j(t) + \omega_j^2\, u_j(t) = -f(t). \tag{14}$$

where $f(t)$ is the ground acceleration and ζ_0 is the relative damping which will be taken hereafter always equal to 5%. The ERS in terms of pseudo-acceleration (PA) is given by:

$$S_{\text{PA}}(T_j) = \omega_j^2 \max_{0 \le \ell \le N_t} \{|u_j(t_\ell)|\}, \tag{15}$$

and we define the ToM spectrum as:

$$S_{\text{ToM}}(T_j) = \tau_j \qquad \Leftrightarrow \qquad S_{\text{PA}}(T_j) = \omega_j^2\, |u_j(\tau_j)|. \tag{16}$$

where $t_\ell = \ell \Delta t$ is the ℓth the $N_t = t_f/\Delta t$ discrete time instants at which the response is computed, Δt being the sampling interval. The ERS and the ToM spectrum are calculated for N_T frequencies, taken from the discrete frequencies of the signal, which are $\omega_j = j\, \Delta\omega$ with j going from 1 to $N_t/2$, in the range of periods where compatibility is of interest ($0.1 \le T_j \le 4.0$s in this study) and $\Delta\omega = 2\pi/(t_f)$. We assume the duration of the transient response of the SDoF oscillator to be ended when its contribution is less then 5% of the stationary response amplitude [15], namely when $t > \Delta\tau(\omega_j) = 3/(\zeta_0 \omega_j)$.

3.2 Proposed algorithm

The first step of the proposed matching procedure is to scale the natural accelerogram by a convenient factor [16] given by:

$$\alpha^{(0)} = \underset{\alpha>0}{\arg\min} \left\{ \sqrt{\frac{1}{N_T} \sum_{j=1}^{N_T} \left(\frac{\alpha\, S_{\text{PA}}^{(0)}(T_j) - S_{\text{ED}}(T_j)}{S_{\text{ED}}(T_j)} \right)^2} \right\}, \tag{17}$$

which leads to minimise the root mean square (RMS) discrepancy between EDS given by the code, S_{ED}, and the ERS of the selected accelerogram, S_{PA}, at the 0th iteration. The method then proceeds with iterations until the code specifications of spectrum compatibility are met. The generic rth iteration requires the following five steps:

1. The current/target spectral ratios are computed:

$$R_j^{(r)} = \min \left\{ \frac{S_{\text{PA}}^{(r)}(T_j)}{S_{\text{ED}}^{\flat}(T_j)}, \frac{S_{\text{ED}}^{\sharp}(T_j)}{S_{\text{PA}}^{(r)}(T_j)} \right\} \tag{18}$$

   where $S_{\text{ED}}^{\flat}(T_j)$ and $S_{\text{ED}}^{\sharp}(T_j)$ are the target EDS, multiplied respectively by 0.9 and 1.3 to obtain the compatibility zone boundaries, and $S_{\text{PA}}^{(r)}(T_j)$ is the ERS related to the signal at the current iteration. If all $R_j^{(r)} \geq 1$, then the spectrum-compatibility is achieved and no further iterations are needed. If not, the worst point in terms of bounded spectral compatibility in the range of interest is found as:

$$j^* = \underset{1 \leq j \leq N_T}{\arg\min} \{R_j^{(r)}\}. \tag{19}$$

   In this way the iteration will be focused on the point having the biggest relative distance from the bounded zone, and the intervention in the rth iteration will be localised in both time domain around $t = \tau^{(r)} = \tau_{j*}$, and frequency domain around $\omega = \Omega^{(r)} = \omega_{j*}$.

2. The frequency band $[\omega_m^{(r)}, \omega_n^{(r)}]$ to be modified in the current iteration is defined by means of its central frequency $\Omega^{(r)}$ and its bandwidth $B^{(r)}$, given by:

$$B^{(r)} = (N_\omega^{(r)} - 1)\Delta\omega, \tag{20}$$

   and therefore:

$$\omega_m^{(r)} = \Omega^{(r)} - B^{(r)}/2; \qquad \omega_n^{(r)} = \Omega^{(r)} + B^{(r)}/2, \tag{21}$$

   with the conditions:

$$N_\omega^{(r)} \geq N_{\omega,\text{min}}; \qquad \frac{2\pi}{\omega_m^{(r)}} - \frac{2\pi}{\omega_n^{(r)}} \geq \Delta T_{\text{min}}, \tag{22}$$

   leading to have a minimum bandwidth of $N_{\omega,\text{min}}$ discrete frequencies or a minimum size ΔT_{min} in terms of natural periods. The two parameters have to be chosen properly to improve the effectiveness of the iterative scheme, and more details are offered in the following.

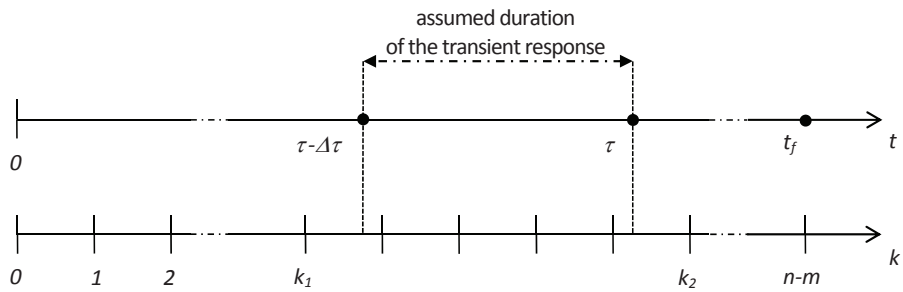

Figure 3: k_1, k_2 definition

3. The sub-signal on which the correction factor will be applied is localised in both time and frequency domains. Firstly, the wavelet transform coefficients $\hat{a}^{(r)}_{\{m^{(r)},n^{(r)}\},k}$ are calculated by a discrete convolution of the signal $f^{(r)}(t)$ with the modifying band wavelets $\hat{\psi}_{\{m^{(r)},n^{(r)}\},k}(t/t_f)$:

$$\hat{a}^{(r)}_{\{m^{(r)},n^{(r)}\},k} = \sum_{\ell=0}^{N_t} f^{(r)}_{\ell}\, \hat{\psi}_{\{m^{(r)},n^{(r)}\},k}\left(\frac{t_\ell}{t_f}\right); \qquad k = 1, ..., (n-m), \tag{23}$$

then the sub-signal is obtained as:

$$\tilde{f}^{(r)}(t) = 2\,\mathrm{Re}\left\{\sum_{k=k_1^{(r)}}^{k_2^{(r)}} \hat{a}^{(r)}_{\{m^{(r)},n^{(r)}\},k}\, \hat{\psi}_{\{m^{(r)},n^{(r)}\},k}\left(\frac{t}{t_f}\right)\right\} \tag{24}$$

which is a summation of the wavelets weighted with the HWT coefficients $\hat{a}^{(r)}_{\{m^{(r)},n^{(r)}\},k}$, and limited for k in the interval $[k_1^{(r)}, k_2^{(r)}]$. It is worth noting that $k_2^{(r)} \leq n^{(r)} - m^{(r)}$ and $k_1^{(r)} \geq 0$, and they can be evaluated as:

$$k_2^{(r)} = \mathrm{int}\left\{\frac{\tau^{(r)}}{t_f}(n^{(r)} - m^{(r)})\right\} + 1; \tag{25}$$

$$k_1^{(r)} = k_2^{(r)} - \mathrm{int}\left\{\frac{\Delta\tau^{(r)}}{t_f}(n^{(r)} - m^{(r)})\right\} + 1; \tag{26}$$

meaning that the time interval in which the bulk of the modification occurs ideally ends at the first k index after the time of maximum response $\tau^{(r)} = S_{\mathrm{ToM}}(2\pi/\Omega^{(r)})$ and begins at the first k index before it, minus the conventional transient duration $\Delta\tau^{(r)} = \Delta\tau(\Omega^{(r)})$ (see Fig. 3).

4. The displacement response $\tilde{u}^{(r)}_{j*}(t)$ can be evaluated by solving the equation:

$$\ddot{\tilde{u}}^{(r)}_{j*}(t) + 2\,\zeta_0\,\omega_{j*}\,\dot{\tilde{u}}^{(r)}_{j*}(t) + \omega^2_{j*}\tilde{u}^{(r)}_{j*}(t) = -\tilde{f}^{(r)}(t), \tag{27}$$

which rules the seismic vibration of a SDoF linear oscillator having the natural circular frequency $\Omega^{(r)}$ and subjected to the sub-signal $\tilde{f}^{(r)}(t)$. Then a product function is defined by:

$$P_{\ell}^{(r)} = u_{j*,\ell}^{(r)} \, \tilde{u}_{j*,\ell}^{(r)}, \tag{28}$$

whose maximum value is sought as:

$$\ell^* = \underset{0 \le \ell \le N_t}{\arg\max} \{ P_{\ell}^{(r)} \} \tag{29}$$

which therefore delivers the value ℓ^* for which the product function between the response to the current signal, $f^{(r)}(t)$, and the response to the current sub-signal, $\tilde{f}^{(r)}(t)$ takes the maximum.

5. The correction factor for the rth iteration is calculated by:

$$\alpha^{(r)} = \frac{D^{(r)} - u_{j*,\ell^*}^{(r)}}{\tilde{u}_{j*,\ell^*}^{(r)}}, \tag{30}$$

where:

$$D^{(r)} = \frac{1}{(\Omega^{(r)})^2} \begin{cases} 1.05 S_{\text{ED}}^{\flat}(T_{j*}^{(r)}) & \text{if} \quad S_{\text{ED}}(T_{j*}^{(r)}) > S_{\text{PA}}^{(r)}(T_{j*}^{(r)}); \\ 0.95 S_{\text{ED}}^{\sharp}(T_{j*}^{(r)}) & \text{if} \quad S_{\text{ED}}(T_{j*}^{(r)}) < S_{\text{PA}}^{(r)}(T_{j*}^{(r)}); \end{cases} \tag{31}$$

with $T_{j*}^{(r)} = 2\pi/(\Omega^{(r)})$. The modified signal at the present iteration is finally found as:

$$f^{(r+1)}(t) = f^{(r)}(t) + \alpha^{(r)} \, \tilde{f}^{(r)}(t), \tag{32}$$

and the next iteration can begin.

It is worth noting here that the last step is based on the superposition principle, as at the generic time instant the total response will be given by the summation of the responses to the two separate inputs, the signal and its time-frequency jointly-localised component. Since the latter component has been related to the spectral value being adjusted both in time and frequency domain, it is likely the best correlation between the two separate responses is achieved at the instant of maximum product. Computing the product function $P_{\ell}^{(r)}$ is therefore necessary to ensure that the modification will have the desired effect on the signal. It happens that up-modification always works, while the down-modification sometimes fails to reduce the spectral value to the desired level. In fact, while the response peak affecting the spectral value is reduced, there could be another peak located somewhere else on the time axis. Nonetheless, by numerical testing, we found a satisfactory rate of success in down-modification, of about 95%. It may be worth emphasising here that in Eq. (30) we do not take into account the difference between the target spectrum value and the current iteration spectrum value, but we consider the response absolute value of the related SDoF oscillator at the instant of maximum product ℓ^* and generally, in terms of displacement spectrum, $S_{\text{D}}^{(r)}(T_{j*}^{(r)}) = S_{\text{PA}}^{(r)}(T_{j*}^{(r)})/(\Omega^{(r)})^2 > u_{j*,\ell^*}^{(r)}$. During extensive numerical testing this scheme has been proved to be very effective.

3.3 Discussion

The presented algorithm can effectively adjust spectral response values by means of modifications localised both in the time and in frequency domain. Despite that, its capability of matching a spectral bounded zone on a range of periods of interest does not follow trivially, especially as ideally the EDS matching should be achieved with a reasonable number of iterations. The fact is that, because of the dispersion of the dynamic amplification function around the natural frequency of the SDoF oscillator, the adjustment brought to a value on the spectrum affects significantly those in its neighborhood too.

Moreover, focusing on time domain, we notice that, despite harmonic wavelets have localisation capabilities, these functions are centred on discrete points which usually do not match with the points where the original signal needs to be modified. As a result, when the original ERS presents sharp peaks, the procedure may encounter difficulties to fit it in a bounded zone on a wide range of periods. Stalling in convergence may sometimes be caused by a sort of ping-pong effect, i.e. the algorithm spends several iterations attempting to fit the spectrum in a certain range: every time it does an up-modification, a down-modification is necessary in the next iteration for a very close value, almost nullifying the effect of the preceding adjustment, and so on. This problem can be overcome by a proper choice of the parameters $N_{\omega,\text{min}}$ and ΔT_{min}, which rule the size of the band subjected to modification (see step (2) above). It should be noted that these two parameters affect different ranges: because of the constant angular frequency discretisation scheme ($\omega_j = j\,\Delta\omega$), $N_{\omega,\text{min}}$ limits the bandwidth in the long periods range, while ΔT_{min} affects the shorts periods range.

Bearing in mind that a compromise between time and frequency domain localisation must be accepted, several schemes were tested for the definition of the frequency band for the generic modification. The idea of the worst band rather then the worst value (sought in step (1)) was also considered, attempting to adjust the widest possible band at every step. While it was potentially capable of reducing the number of iterations needed, the drawbacks associated with this approach were the implementation complexity and the lack of a meaningful central frequency for the computation of the modification factor, which eventually let us prefer the scheme of steps (1-2) above.

3.4 Numerical examples

In order to assess the effectiveness of the proposed procedure, several recorded accelerograms were studied to cover different scenarios. The proposed HWT-based method was used to fit them on the Eurocode (EC8) spectral shapes for a peak ground acceleration (PGA) of 0.36 g, considering the best and the worst initial matching in terms of RMS discrepancy (Eq. (17)). As a term of comparison, a FT-based method was implemented by means of the same algorithm described in the preceding section, but modified in step (3) letting $k_1 = 0, k_2 = N_t/(n-m)$, which means that all k-indexed coefficients of a wavelets train are used, and hence no time localisation is achieved. By doing this, we can quantify the advantages of the time localisation capa-

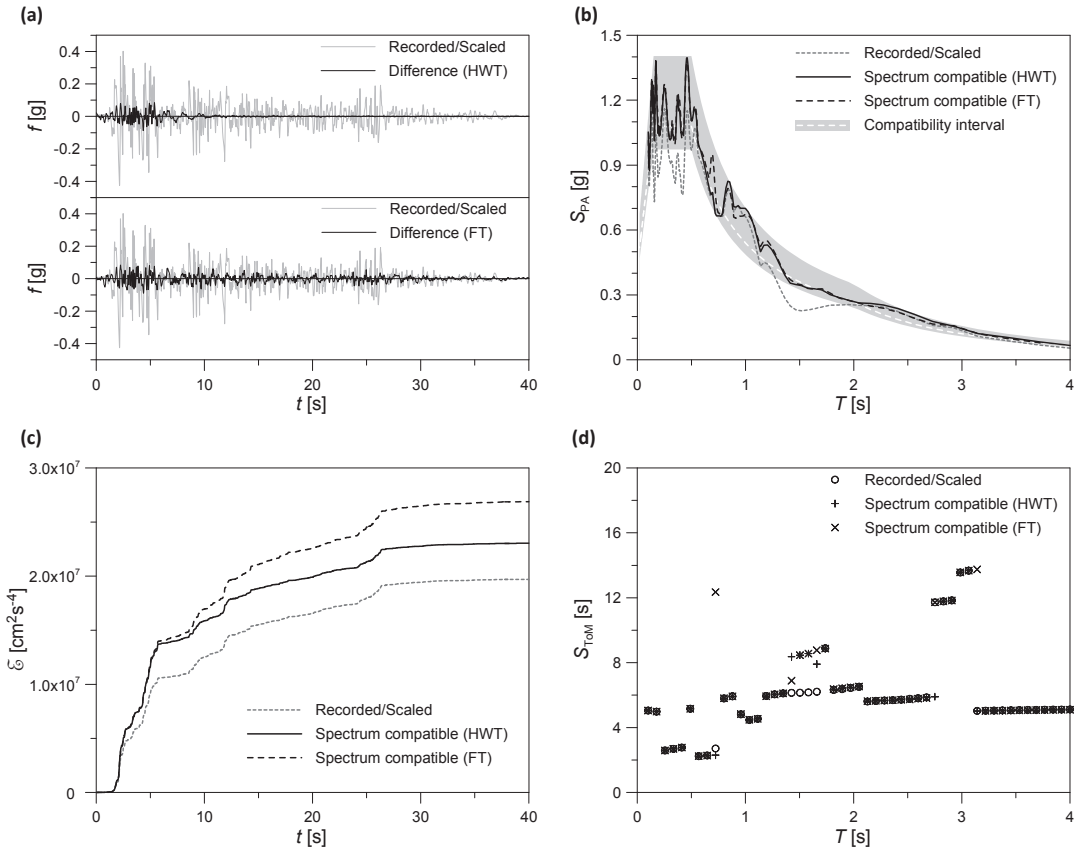

Figure 4: Elcentro, matching with EC8 soil B spectral shape (best matching)

bilities of the HWT over the FT, in bringing the minimum modification to the original record.

Due to the space limitation, the results are presented herein for just three accelerograms, whose main characteristics (sample interval, moment magnitude, focal depth and Joyner-Boore distance, PGA) are listed in Table 1. The El Centro record has been considered because its ERS closely resembles the EC8 EDS shapes. The best in terms of initial RMS matching (Eq. (17)) with EC8 spectral shapes is the soil type B (see Table 2 and Fig. 4), and the advantage of the proposed HWT-based procedure over an FT-based approach is apparent considering that the energy content rise due to the modification (ΔE) is less than a half. The Erzincan accelerogram has been chosen as

earthquake	*site/component*	Δt[s]	M_w	depth/dist[km]	PGA[g]
Imperial Valley 1940	ElCentro/N-S	0.010	7.0	8.80 / 6.09	0.258
Erzincan 1992	Erzincan/E-W	0.005	6.7	27.00 / 0.00	0.495
Irpinia 1980	Calitri /E-W	0.005	6.9	15.00 / 13.30	0.175

Table 1: Cases of study

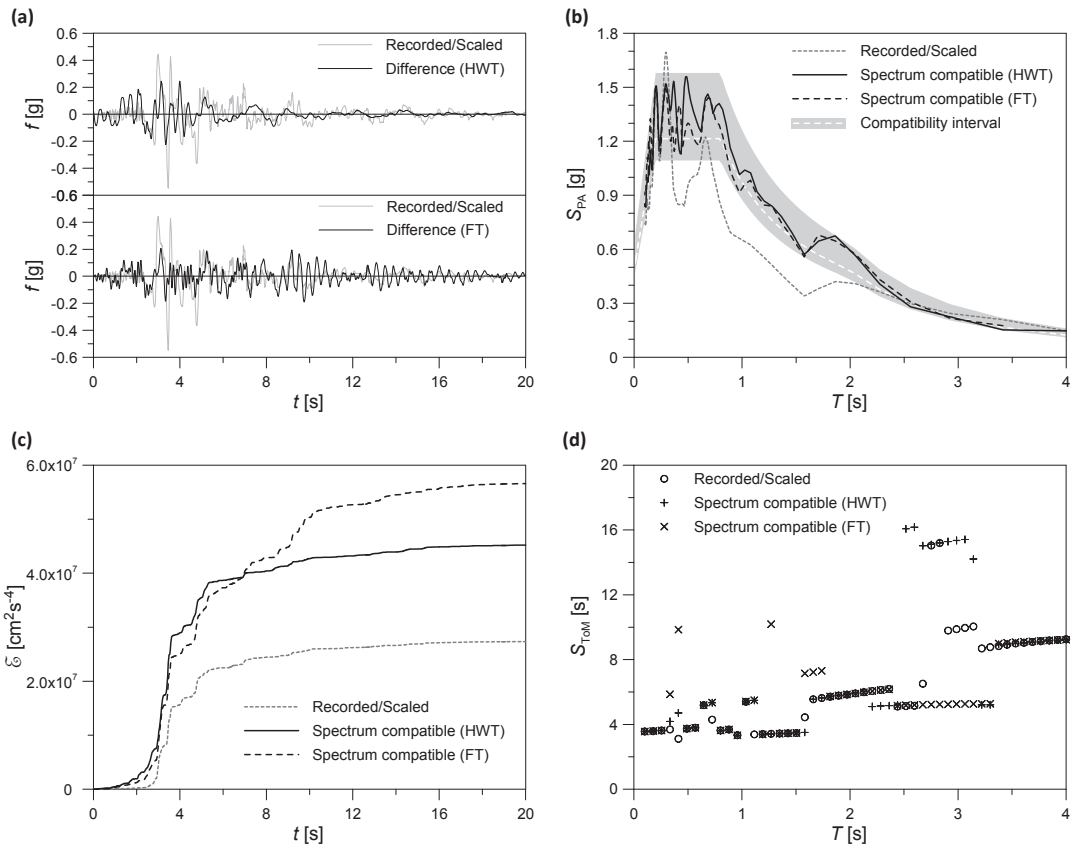

Figure 5: Erzincan, matching with EC8 soil D spectral shape (best matching)

an example of near-fault record, characterised by an impulse in terms of ground velocity and displacement and also in this case the best initial RMS matching (with EC8 soil type D) has been considered. Finally, the Irpinia record has been selected because of its peculiar nature showing a double intense phase, due to a two-stage fault rupture. In this case the results are shown for the worst matching spectral shape (A), providing an example of the effectiveness of the procedure in the most challenging scenario.

In all the three cases, the performance of the proposed HWT-based correction, due to its joint localisation in time and frequency, is better than the FT-based correction, for which the increase in the total energy of the signal, ΔE, is doubled, meaning that more modifications have been introduced to achieve the spectrum-compatibility requirement, and hence the original characteristics of the accelerograms have been more heavily affected. This clearly emerges also from a close look at the time histories reported in sub-graphs (a) of Figs. 4 to 6, showing that the iterations are much more localised in the HWT-based procedure, and in sub-graphs (c) as well, plotting the cumulated energy of the signal, which raises further for the FT-based procedure. Sub-graphs (b) show that both HWT and FT allow achieving the compatibility with the target spectrum, even if the original ERS (recorded/scaled) and the EDS supplied by the building code have very different shapes (see in particular Fig. 6(b)). Sub-

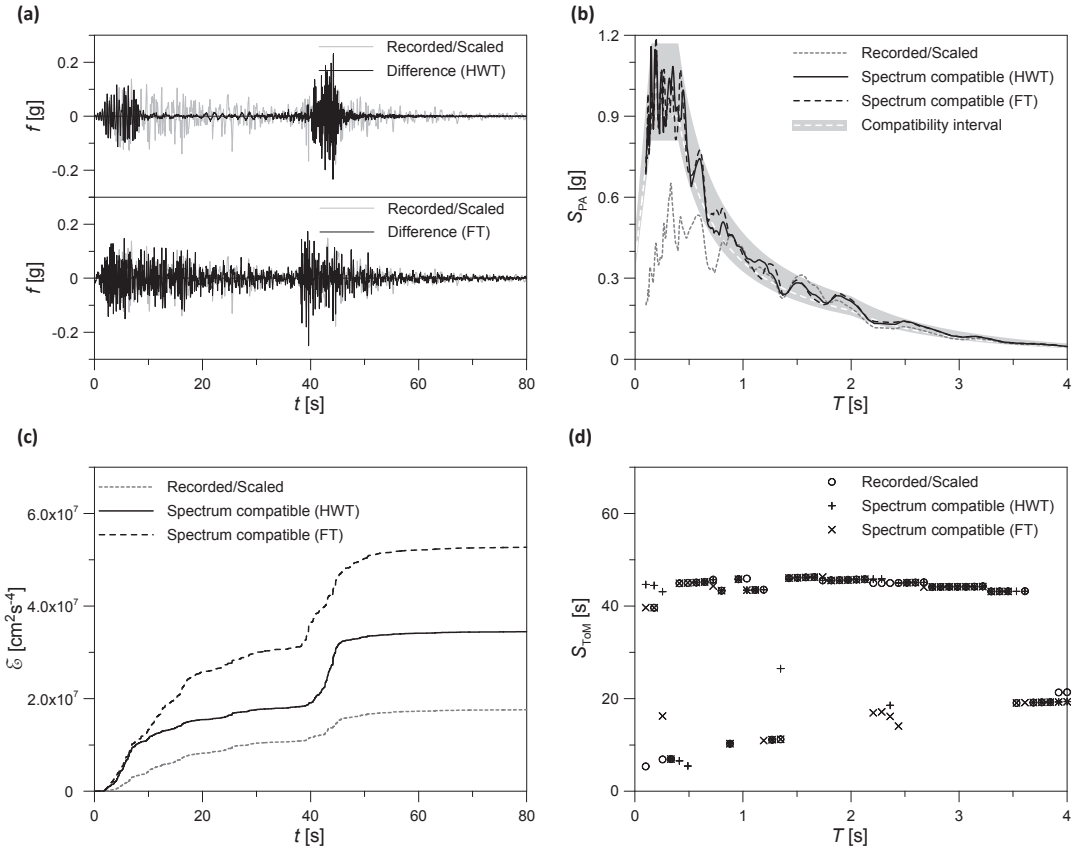

Figure 6: Irpinia, matching with EC8 soil A spectral shape (worst matching)

graphs (d) show the ToM spectra, and once again the HWT has to be preferred since the FT tends to disturb much more the original distribution of the times of response maximum. From a close look at Figs. 4 to 6(a), it is apparent how the correction applied to the signal (difference) is localised in the case of the proposed method, while it is spread over the overall duration for the FT-based procedure. As a result the energy increase is much smaller (Figs. 4 to 6(c)). Figs. 4 to 6(b) show how both methods manage to fit the spectrum in the target zone, while from Figs. (d) it can be seen that the proposed method brings a smaller modification in terms of time instants when the maxima of the response are experienced.

				FT		HWT	
earthquake	*target shape*	α_0	RMS_0	ΔE	RMS_f	ΔE	RMS_f
ElCentro	B (best)	1.361	0.162	+36.4%	0.132	+16.9%	0.152
Erzincan	D (best)	1.106	0.237	+107.1%	0.137	+46.3%	0.140
Irpinia	A (worst)	1.017	0.208	+201.9%	0.157	+68.7%	0.136

Table 2: matching details

4 Stochastic generation procedure

In the field of stochastic time history generation, a typical approach is to: firstly, assess a function capable of describing the features of interest about the phenomenon being simulated, in terms of time-evolving frequency and amplitude; secondly, use a generation procedure to obtain the needed samples. The main difficulty is to describe with the same function both time and frequency domain features, which inevitably need a compromise due to the Heisenberg's uncertainty principle. In the case of seismic ground motions other difficulties arise because of the lack of records in such a quantity to do statistically reliable assessment on the phenomenon. For this reason we propose a stochastic generation procedure that allows generating the samples without the need to formulate a spectral function. A common practice (see [5] and [17]) for generating a sample of a stationary Gaussian process is summing a great number N of cosine wave with random phases:

$$f(t) = \sqrt{2} \sum_{j=1}^{N} \sqrt{2 S_{ff}(\omega_j)\, \Delta\omega}\, \cos(\omega_j t + \phi_j), \tag{33}$$

where $S_{ff}(\omega)$ is the power spectral density of the random process, ϕ_j are a set of independent random variables uniformly distributed on $[0, 2\pi)$, $j = 1, 2, ..., N$, $\omega_j = j\Delta\omega$, and $f(t)$ is a generated sample. Note that the simulated process is asymptotically gaussian as N becomes large due to the central limit theorem. The samples can be modulated afterwards by using a deterministic function $A(t)$, but the frequency content will remain stationary. A straightforward extension of the (33) to the non-stationary case is provided by:

$$f(t) = \sqrt{2} \sum_{j=1}^{N} \sqrt{2 A^2(t, \omega_j) S_{ff}(\omega_j)\, \Delta\omega}\, \cos(\omega_j t + \phi_j), \tag{34}$$

where $A^2(t, \omega)$ is the the non-stationary amplitude and frequency content.

As a natural extension of this traditional procedure, in this study the performance of a phase angle rotation of the harmonic wavelets to achieve the randomisation of the present signal has been investigated. To do this, 2,000 samples have been generated starting from the spectrum-compatibilised El Centro 1940 accelerogram by using the dyadic (see Eqs. (6) to (8)) phase randomisation procedure. Fig. 7(a) compares the parent signal (gray line) and a generic sample (black line), and the magnified time interval shows that the two time histories are quite similar, meaning that the HWT-based generation method adopted for this accelerogram has not altered characteristically the parent time history, therefore preserving most of its non-stationary characteristic. This consideration is confirmed by the standard deviation of the 2,000 samples (Fig. 7(c)), which mirrors quite closely the envelope of the parent signal, and average of the corresponding 2,000 FT spectra (Fig. 7(d)), which shows a peculiar piece-wise constant distribution, i.e. the HWT-based randomisation tends to uniformly distribute the energy level in each frequency band determined by the Newland's dyadic scheme (see

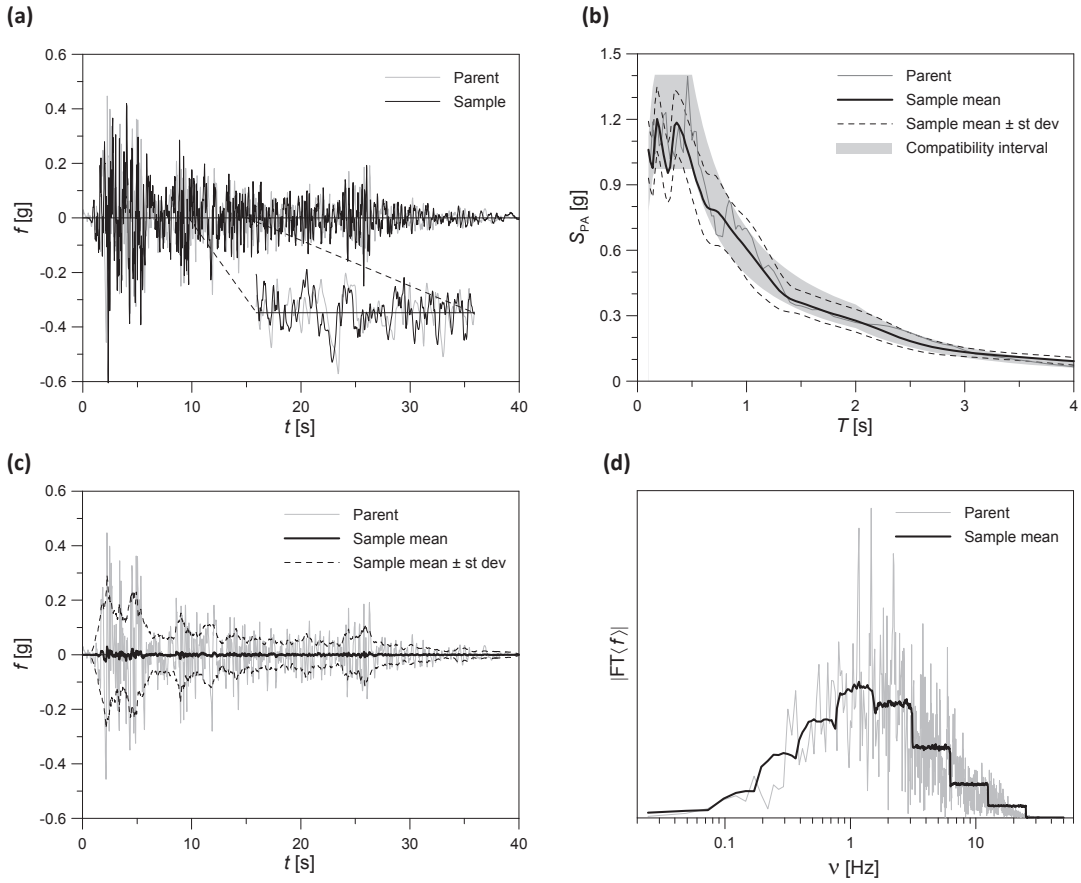

Figure 7: HWT dyadic phase randomisation

Fig. 1(a)). It can be also observed that the 2,000 samples compare very well with the target EDS in terms of average (solid line in Fig. 7(b)), while showing their statistical dispersion (dashed line in Fig. 7(b)) can be perceived as acceptable (at least within the linear range) for earthquake engineering applications. Further investigations, however, will be required to assess the effects on different types of non-linear structural behaviour.

It is worth stressing here that the proposed HWT-based procedure can be seen as a sort of optimal compromise, in terms of the emphasis in preserving the parent's information in either time domain or frequency domain. As a matter of fact, adopting an extreme approach, focused on just one of the two domain, is not able of deliver useful results for seismic design purposes. To further highlight this point, Figs. 8 and 9 show the results obtained by preserving untouched the available information either in the frequency domain or in the time domain, respectively. In the first case, the 2,000 samples show a deterministic FT spectrum (Fig. 8(d)), i.e. the frequency content is perfectly preserved, by they become realisation of a stationary random process (Fig. 8(c)). The opposite happens in the second case, where the time history of the parent ground acceleration is used as a deterministic modulating function of random white noise (Fig. 8(d)). Interestingly, in both cases the average ERS fails to satisfy

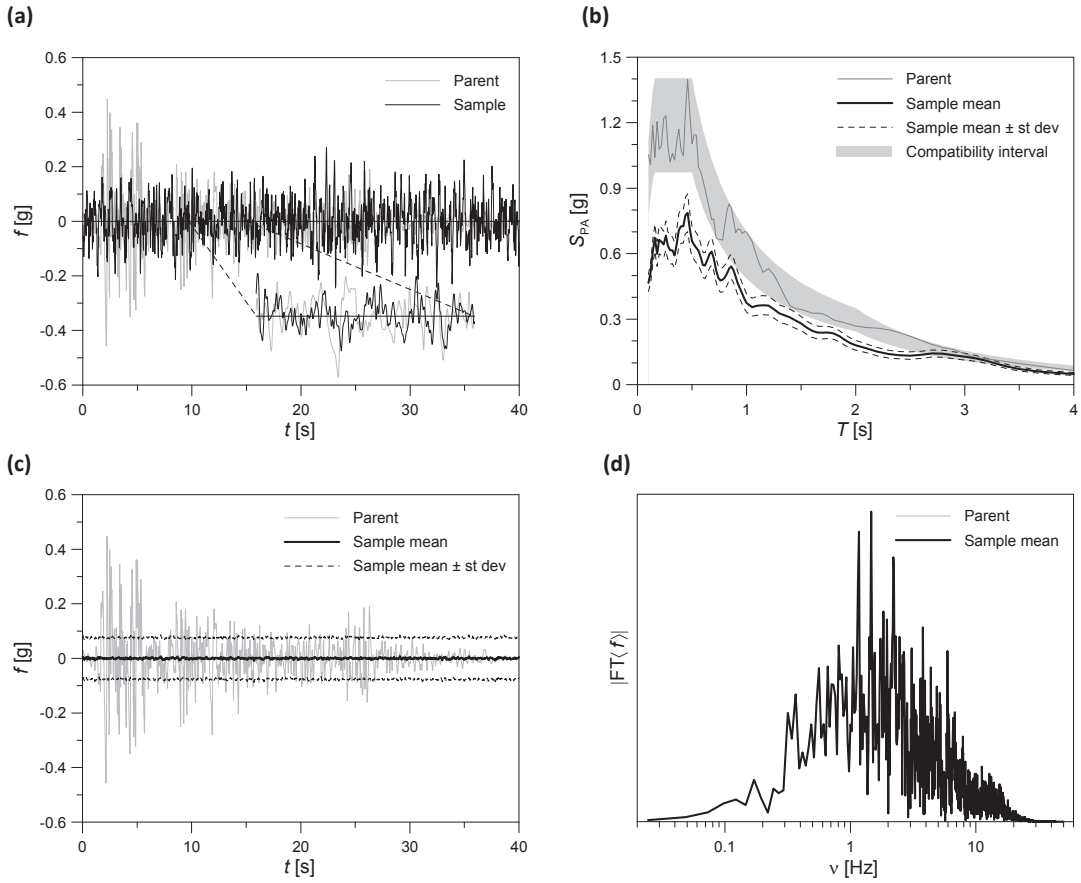

Figure 8: FT phase randomisation

the spectrum-compatibility requirement, which is a further proof that both time and frequency domain bear useful information for the purpose of the seismic analysis of structures.

5 Concluding remarks

In this paper, the HWT was found to be a very powerful tool for dealing with seismic signals and their inherent non-stationarity, both in terms of amplitude and frequency content, which in turn may play a crucial role for the purposes of analysis and design of earthquake-resistant structures. Since the HWT allows a joint time-frequency representation and manipulation of signals, two new procedures have been proposed, which can be readily used: first, a deterministic modification method, aimed at achieving the spectral matching of a given accelerogram to a target EDS; second, a stochastic generation procedure, which randomises a parent signal to get an arbitrary number of samples with similar non-stationary characteristics.

It has been shown that the spectral matching method, working in an iterative way, brings modifications to the signal which are localised both in time and frequency do-

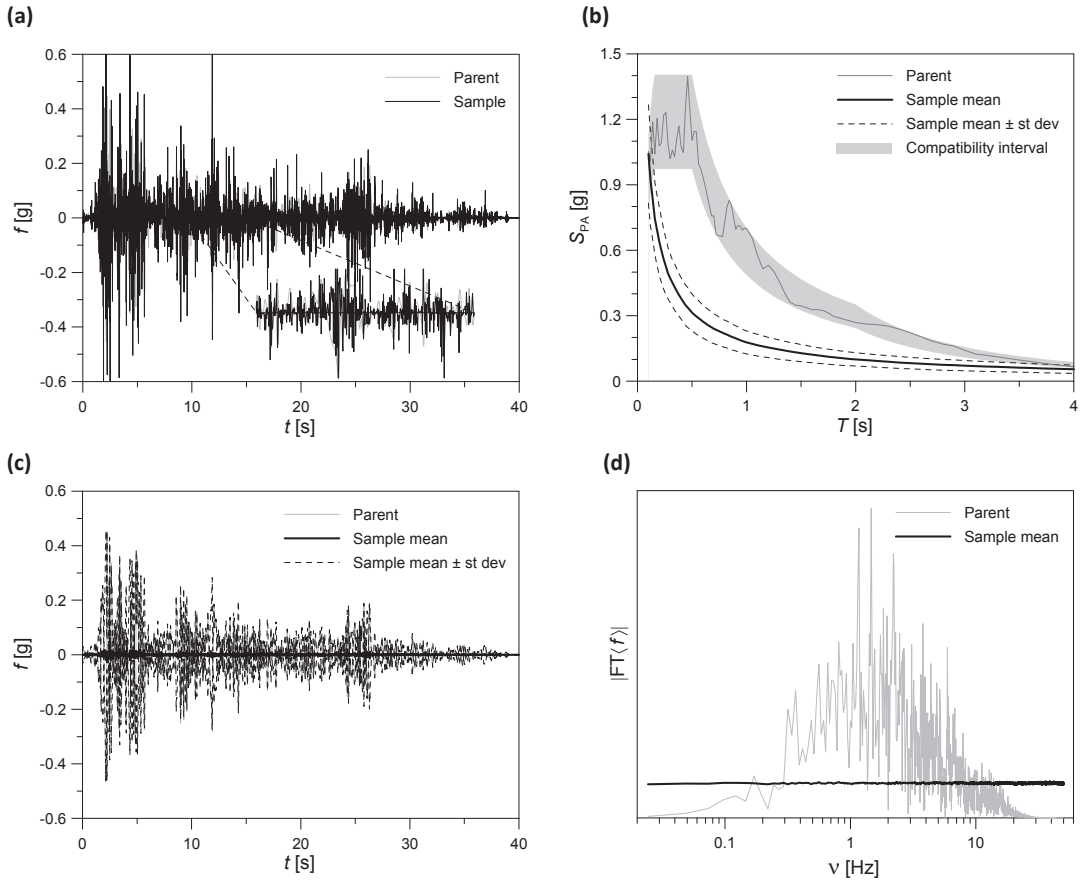

Figure 9: WN multiplication

main, and for this reason is able to achieve the required spectral compatibility with minimum modification in terms of additional energy content. It has been also shown that the randomisation method, consisting of a phase angle rotation of the wavelets, allows generating the required number of fully non-stationary samples without the need of defying the evolutionary power spectral density of the ground acceleration, and provides an effective compromise while retaining information from both time and frequency domain.

Extensive numerical investigations have demonstrated the excellent performance of the proposed methods, particularly in comparison with the results achievable with a traditional FT-based approach. Further study will be required to ascertain the effects of the HWT-based modification and generation on the seismic response of non-linear structures.

References

[1] E.I. Katsanos, A.G. Sextos, and G.D. Manolis, “Selection of earthquake ground motion records: A state-of-the-art review from a structural engineering perspec-

tive", Soil Dynamics and Earthquake Engineering, vol. 30, pp. 157-169, 2010.
[2] A. Zerva, "Seismic source mechanisms and ground motion models", Probabilistic Engineering Mechanics, vol. 3,no. 2, pp. 64-74, 1988.
[3] N. Lam, J. Wilson, ans G. Hutchinson, "Generation of synthetic earthquake accelerograms using seismological modelling: a review", Journal of Earthquake Engineering, vol. 4, no. 3, pp. 321-354, 2000.
[4] D. Gasparini and E. Vanmarke, "Simulated earthquake motions compatible with prescribed response spectra", publication no. r76-4, tech. rep., Massachusetts Institute of Technology (MIT), Department of Civil Engineering, 1976.
[5] M. Shinozuka and G. Deodatis, "Stochastic process models for earthquake ground motion", Probabilistic Engineering Mechanics, vol. 3, no. 3, pp. 114-123, 1988.
[6] A. Giaralis and P. Spanos, "Wavelet-based response spectrum compatible synthesis of accelerograms-eurocode application (EC8)", Soil Dynamics and Earthquake Engineering, vol. 29, no. 1, pp. 219-235, 2009.
[7] F. Sabetta and A. Pugliese, "Estimation of response spectra and simulation of nonstationary earthquake ground motions", Bulletin of the Seismological Society of America, vol. 86, no. 2, pp. 337-352, 1996.
[8] S. Rezaeian and A. D. Kiureghian, "Simulation of synthetic ground motions for specified earthquake and site characteristics", Earthquake Engineering and Structural Dynamics, vol. 39, no. 10, pp. 1155-1180, 2010.
[9] P. Cacciola, "A stochastic approach for generating spectrum compatible fully non-stationary earthquakes", Computers and Structures, vol. 88, no. 15-16, pp. 889-901,2010.
[10] J.J. Bommer, A.B. Acevedo, "The use of real earthquake accelerograms as input to dynamic analysis", Journal of Earthquake Engineering, vol. 8:s1, pp. 43-91, 2004.
[11] P. Schwab, P. Lestuzzi, "Assessment of the seismic non-linear behavior of ductile structures due to synthetic earthquakes", Bulletin Earthquake Engineering, vol. 5, no.1, 2007.
[12] S. Mallat, "A wavelet tour of signal processing: the sparse way", Elsevier /Academic
[13] D. Newland, "Harmonic wavelet analysis", Proc. R. Soc. Lond. A, vol. 443, pp. 203-225, 1993.
[14] D. Newland, "Harmonic and musical wavelet", Proc. R. Soc. Lond. A, vol. 444, pp. 605-620, 1994.
[15] G. Muscolino, "Dinamica delle Strutture", The Mcgraw-Hill Companies, 2003.
[16] I. Iervolino, C. Galasso, and E. Cosenza, "Rexel: Computer aided record selection for code-based seismic structural analysis", Bulletin of Earthquake Engineering, vol. 8, no. 2, pp. 339-362, 2010.
[17] M. Shinozuka and G. Deodatis, "Simulation of stochastic processes by spectral representation", Applied Mechanics Reviews, vol. 44, no. 4, pp. 191-204, 1991.